

RSC Advances



This is an *Accepted Manuscript*, which has been through the Royal Society of Chemistry peer review process and has been accepted for publication.

Accepted Manuscripts are published online shortly after acceptance, before technical editing, formatting and proof reading. Using this free service, authors can make their results available to the community, in citable form, before we publish the edited article. This *Accepted Manuscript* will be replaced by the edited, formatted and paginated article as soon as this is available.

You can find more information about *Accepted Manuscripts* in the [Information for Authors](#).

Please note that technical editing may introduce minor changes to the text and/or graphics, which may alter content. The journal's standard [Terms & Conditions](#) and the [Ethical guidelines](#) still apply. In no event shall the Royal Society of Chemistry be held responsible for any errors or omissions in this *Accepted Manuscript* or any consequences arising from the use of any information it contains.



COMMUNICATION

Space Charge-Induced Unusually-High Mobility of Solution-Processed Indium Oxide Thin Film Transistor with Ethylene Glycol Incorporated Aluminum Oxide Gate Dielectric

Received 00th January 20xx,
Accepted 00th January 20xx

DOI: 10.1039/x0xx00000x

www.rsc.org/advances

Hyungjin Park[‡], Yunyong Nam[‡], Jungho Jin^b, and Byeong-Soo Bae^{a*}

The incorporation of ethylene glycol (EG) into a high-k aluminium oxide gate dielectric layer was achieved by solution process, leading to a distinct increase in the mobility of indium oxide TFT. Frequency-dependent capacitance originated from residual EG was examined and accompanying effects on indium oxide TFT were studied.

Oxide thin film transistors (TFTs) have been widely studied as an element of the driving and switching circuits for flat panel, flexible, and transparent displays. A metal oxide semiconductor (MOS) as a channel layer has various advantages, including transparency, large area reproducibility, and high stability, as well as good electrical characteristics. Although carrier mobilities of MOSs are generally much higher than those of amorphous silicon semiconductors ($\sim 1 \text{ cm}^2 \text{ V}^{-1} \text{ s}^{-1}$), in order to achieve high-definition and high-resolution displays, the MOSs must afford comparable mobility with low temperature poly-silicon (over $100 \text{ cm}^2 \text{ V}^{-1} \text{ s}^{-1}$) for high-speed driving¹. In this regard, various processing techniques have been studied to improve the electrical properties of the semiconductor layer, composed of indium zinc oxide (IZO), indium gallium zinc oxide (IGZO), indium oxide (In_2O_3), or zinc tin oxide (ZTO).²⁻⁷ However, MOS channel layers deposited on the conventional silicon dioxide (SiO_2) as the gate dielectric have shown a limited mobility of up to around $40 \text{ cm}^2 \text{ V}^{-1} \text{ s}^{-1}$.⁸ Recent research in this area has focused on improving TFT performance by introducing various gate dielectrics. Since the gate dielectric layer adheres to the electron channel generated from the semiconductor layer, its structural and electrical properties significantly affect the TFT performance. Requisites of the gate dielectric for high performance are a smooth

surface and compatibility with semiconductor materials while simultaneously offering good insulating properties such as a wide band gap and high capacitance. In particular, high capacitance of the dielectric layer (high-k) readily attracts carrier electrons under a low gate bias, resulting in a high on-current and mobility.⁹⁻¹⁰ Zhang *et al.* showed a high mobility of $40.5 \text{ cm}^2 \text{ V}^{-1} \text{ s}^{-1}$ using sputtering Ta_2O_5 as the gate dielectric in a ZnO TFT.¹¹ Park *et al.* reported a solution-processed indium oxide (In_2O_3) TFT with a boron (B) doped ZrO_2 dielectric ($k \sim 12.1$) with a mobility of $39.3 \text{ cm}^2 \text{ V}^{-1} \text{ s}^{-1}$ through 250°C annealing, whereas a SiO_2 dielectric ($k \sim 3.9$) based In_2O_3 TFT showed mobility of $15.95 \text{ cm}^2 \text{ V}^{-1} \text{ s}^{-1}$.¹² In addition, even oxide TFTs exhibiting mobility over $100 \text{ cm}^2 \text{ V}^{-1} \text{ s}^{-1}$ using solution-processed AlO_x and YO_x gate dielectrics have been reported.¹³⁻¹⁴

However, notably high mobility, especially with reduced annealing temperature of the dielectric layer seems questionable, because of the defective nature of solution-processed metal oxide layers. The similarity found in literature on high mobility achieved by high-k gate dielectric is that they use a mixture of solvents containing ethylene glycol (EG). EG increases the viscosity of the solution resulting in a thicker gate dielectric layer.^{13, 15-17} Due to a higher boiling point of around 197°C than common solvents such as 2-methoxyethanol ($\sim 124^\circ\text{C}$) and acetonitrile ($\sim 81^\circ\text{C}$), EG may contribute to undecomposed residuals in the layer in a low-temperature process.¹⁸ Another suspicious point is that the manner of calculating mobility from on-current. When a dielectric material contains impurities, the capacitance varies depending on frequency.^{17, 19-20} According to the square-law equation, the capacitance of the gate dielectric is inversely related to the mobility, which raises the importance of choosing an appropriate k value, especially for a high-k gate dielectric.

Herein, we investigate the unusual high mobility observed in metal oxide TFT adopting a solution-processed aluminum oxide (AO) gate dielectric. Precursor solutions with and without EG were designed to track the thermal evolution of the aluminum oxide layer and analyze its electrical properties

^a Laboratory of Optical Materials and Coating (LOMC), Department of Materials Science and Engineering, Korea Advanced Institute of Science and Technology (KAIST), 291 Daehak-ro, Yuseong-gu, Daejeon 305-701, Korea
E-mail: bsbbae@kaist.ac.kr

^b Multiscale Hybrid Materials Laboratory (MHML), School of Materials Science and Engineering, University of Ulsan, 93 Daehak-ro, Nam-gu, Ulsan 680-749, Korea

[†] Electronic Supplementary Information (ESI) available: TGA analyses of precursor solutions. TEM, XRD and AFM data of Al_2O_3 film. See DOI: 10.1039/x0xx00000x
[‡] Equally contributed to this work

at discrete temperature. With an aqueous route indium oxide semiconductor which has the lower annealing temperature than the gate dielectric, the effect of EG in AO gate dielectric on the TFT performance is examined.

The preparation steps for an AO and EG-AO gate dielectric and In_2O_3 TFT are described in Fig. 1. The AO film, as a reference, was prepared by dissolving aluminum nitrate nonahydrate ($\text{Al}(\text{NO}_3)_3 \cdot 9\text{H}_2\text{O}$, 98%, Sigma-Aldrich) in 2-methoxyethanol ($\text{CH}_3\text{OCH}_2\text{CH}_2\text{OH}$, 99.8%, Sigma-Aldrich). For the EG-AO films, aluminum nitrate was dissolved in a mixture of ethylene glycol ($\text{HOCH}_2\text{CH}_2\text{OH}$, 99.8%, Sigma-Aldrich) and 2-methoxyethanol with a 50/50 volume ratio. The molar concentration of the solutions was set to 0.4 M and the solutions were stirred for 6 hours. The precursor solutions were spincoated at 3000 rpm for 25 seconds and dried for 10 minutes at the final annealing temperature. AO film was fabricated by 6 iterative coating and drying cycles and EG-AO films were prepared by 4 cycles to obtain the desired thickness. Finally, spun-on films were annealed at 250, 350, and 500°C for 4 hours in air and referred to as AO 250°C, EG-AO 250, 350, and 500°C. The thicknesses of the AO 250°C, EG-AO 250, 350, and 500°C layers are 190 nm, 155 nm, 110 nm, and 100 nm, respectively (Fig. S1a-d). As the annealing temperature increases, solutions are decomposed and/or evaporated resulting in dense films. The AO and EG-AO films are in an amorphous phase up to 500°C (Fig. S1e) and all the films showed excellent root mean square roughness (R_{RMS}) of 0.187 nm, 0.198 nm, 0.102 nm, and 0.119 nm, respectively, contributing to high insulating ability and a smooth surface (Fig. S2).²¹

Fig. 2 shows the output and transfer characteristic curves of the In_2O_3 TFTs with the AO and EG-AO gate dielectric. An aqueous indium oxide precursor solution was synthesized by

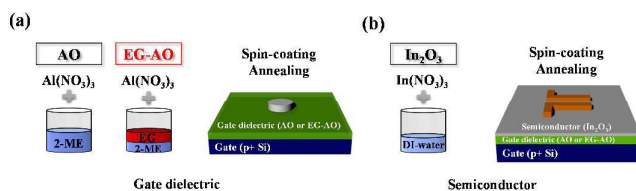


Fig. 1 Schematic illustration for fabrication of (a) MIM device structure using aluminum oxide (AO) or ethylene glycol-incorporated aluminum oxide (EG-AO) gate dielectric and (b) indium oxide TFT based on AO and EG-AO gate dielectric.

dissolving 0.2 M indium nitrate hydrate in de-ionized water.² The synthesized solution was spin-coated on the prepared AO or EG-AO / p+ Si substrate at 5000 rpm for 30 sec. The annealing process was carried out at 250°C for 4 h in air. The Al source and drain electrodes were then deposited on the semiconductor layer by e-beam evaporation with a shadow mask. The thickness of the Al source/drain electrode was 100 nm and the channel width and length were 1000 μm and 100 μm , respectively. All of the In_2O_3 TFTs exhibited clear pinch-off behavior in the output curve. The drain current (I_D) of the In_2O_3 TFT with EG-AO 250°C in the output curve is one order higher than that of the other TFTs. Its transfer characteristics also

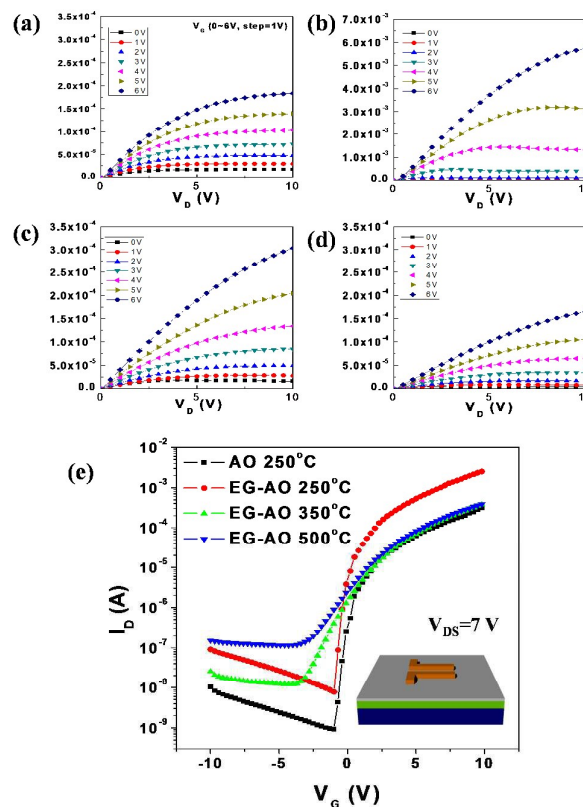


Fig. 2 Output characteristics of solution-processed 250°C In_2O_3 TFTs with (a) AO 250°C, (b) EG-AO 250°C, (c) EG-AO 350°C, and (d) EG-AO 500°C gate dielectric. Range of gate voltage is 0 V to 6 V with a step of 1 V. (e) Transfer curves of In_2O_3 TFTs with AO and EG-AO films prepared at various temperatures as gate dielectrics.

Table 1 Summary of electrical properties of AO and EG-AO dielectric layers annealed at various temperatures and In_2O_3 TFTs prepared using those films as gate dielectrics.

Dielectrics	Capacitance (nFcm^{-2})		Dielectric constant		Mobility ($\text{cm}^2\text{V}^{-1}\text{s}^{-1}$)		I_{ON} (A) at 10V	$I_{\text{ON/OFF}}$	S.S. (V/dec.)
	at 1 Hz ^a	at 1 MHz	at 1 Hz ^a	at 1 MHz	at 1 Hz ^b	at 1 MHz			
AO 250°C	40.5	27	8.7	5.8	19.4	23.1	2.9×10^{-4}	$\sim 10^5$	0.35
EG-AO 250°C	110	35.7	19.2	6.25	46.2	136.4	2.5×10^{-3}	$\sim 10^5$	0.28
EG-AO 350°C	48.3	42.6	6	5.3	25.7	30.5	3.8×10^{-4}	$\sim 10^4$	0.99
EG-AO 500°C	54.9	47.8	6.2	5.4	19.7	23.3	3.7×10^{-4}	$\sim 10^3$	1.2

(a) Obtained from extrapolated capacitance curve

(b) Calculated from capacitance values at 1 Hz

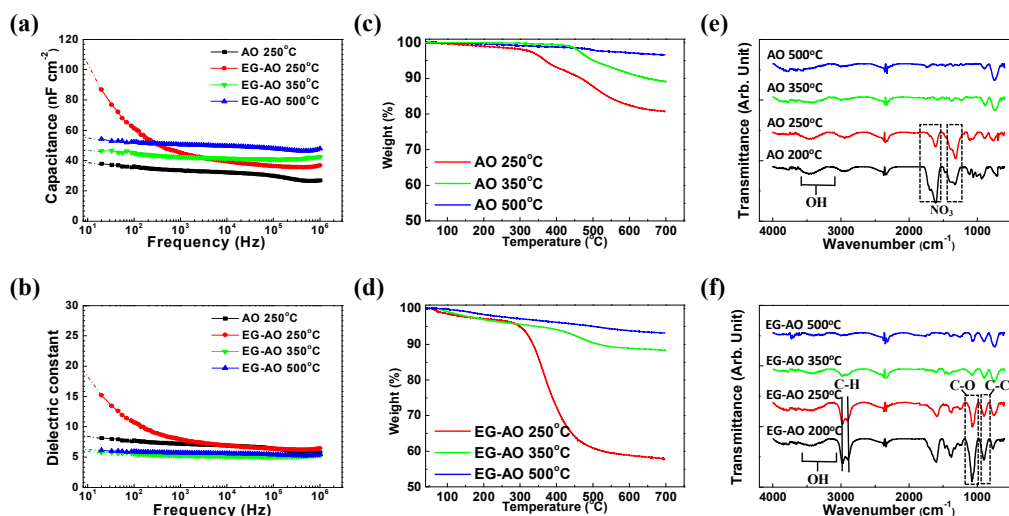


Fig. 3 (a) Capacitance and (b) dielectric constant curves according to frequency of MIM devices fabricated using AO and EG-AO films annealed at various temperatures as insulators. TGA results of (c) AO and (d) EG-AO precursor solutions after annealing at various temperatures for 4 h. The heating rate was 5°C/min. FT-IR spectra of (e) AO and (f) EG-AO films annealed at various temperatures.

show superior electrical results, exhibiting an on-current (I_{ON}) of 2.5×10^{-3} A, an on/off ratio ($I_{ON/OFF}$) of around 10^5 , and a sub-threshold swing (S.S.) of 0.28. The field-effect mobility (μ_{sat}) of the TFTs can be calculated in the saturation region using the following equation:

$$I_{DS} = \frac{W}{2L} \mu C_i (V_G - V_T)^2 \quad (1)$$

where I_{DS} is the drain to the source current, W and L are the width and length of the channel, respectively, C_i is the capacitance per unit area of gate dielectric, V_G is the gate voltage, and V_T is the threshold voltage.

To calculate the mobility of the TFT with each gate dielectric, the capacitance was measured using a metal-insulator-metal (MIM) structure as a function of frequency from 20 Hz to 1 MHz (Fig. 3a). In addition, dielectric constant was obtained using the equation; $C = \epsilon_0 k A/d$, where C is the capacitance of the gate dielectric layer, ϵ_0 is the vacuum permittivity (8.85×10^{-14} Fcm⁻¹), A is the area of the capacitor, and d is the thickness of the dielectric (Fig. 3b). The AO 250°C, EG-AO 350°C, and EG-AO 500°C exhibit a nearly flat capacitance-frequency curve (C-f curve) and constant capacitance over the entire range of frequency. According to the conventional manner in which the capacitance at 1MHz is used for the mobility calculation, the In₂O₃ TFTs with AO 250°C, EG-AO 350°C, and 500°C dielectrics showed mobilities of $23.1 \text{ cm}^2 \text{V}^{-1} \text{s}^{-1}$, $30.5 \text{ cm}^2 \text{V}^{-1} \text{s}^{-1}$, and $23.3 \text{ cm}^2 \text{V}^{-1} \text{s}^{-1}$, respectively. On the other hand, the EG-AO 250°C gate dielectric experiences a frequency-dependent capacitance, especially at a low frequency region. Since the characterization of TFT device is conducted in a static condition, the capacitance value at a low frequency qualifies for extracting representative mobility. While the capacitance at 1 Hz was 110 nFcm^{-2} , where 1 Hz capacitance was assumed by extrapolating to a frequency of 1 Hz from the C-f curve, it significantly decreased to one third (35.7 nFcm^{-2}) as the

frequency increases to 1 MHz.^{17, 19-20} When using capacitance of 1 MHz, the mobility of the EG-AO 250°C based TFT is $136.4 \text{ cm}^2 \text{V}^{-1} \text{s}^{-1}$. Such high mobility is adjusted to $46.2 \text{ cm}^2 \text{V}^{-1} \text{s}^{-1}$ by calculating from k at 1 Hz. The electrical properties of each device is summarized in Table 1.

The frequency-dependent capacitance is clearly observed when EG is included in precursor solution and annealed at temperature lower than 350°C. TGA analysis of EG-AO precursor solution dried at 120°C displays a large amount of weight loss compared with AO precursor solution and the thermal decomposition terminates over 450°C (Fig. S3). Since the only difference between the two samples is the existence of EG in the solution, the noticeable drop in weight is attributed to EG, which has a high onset of decomposition temperature (240°C) and boiling point (197.6°C).¹⁸ Moreover, discrete weight loss over 330°C indicates that high thermal energy is necessary to completely eliminate undecomposed residuals in the EG-AO film.

In order to determine the quantity of the undecomposed portion in the film after the final annealing process, the AO and EG-AO precursor solutions were annealed at 250°C, 350°C, and 500°C for 4 hours and collected for TGA measurement. As presented in Fig. 3c and d, all samples showed negligible weight loss up to each annealing temperature. Beyond the annealing temperatures, the weights gradually decreased up to 700°C. For the samples annealed at 350°C and 500°C, the final weights are around 10%, and 5%, respectively, regardless of whether EG is incorporated. On the other hand, 250°C annealed AO and EG-AO show a large disparity in weight loss over 300°C. The EG-AO 250°C sample ends up having less than 60% of its initial weight, whereas the AO 250°C sample retains around 80% of its weight up to 700°C. Even though most of the weight loss occurs in a range of 300°C to 400°C for EG-AO 250°C, weight loss of EG-AO 350°C and AO 350°C is

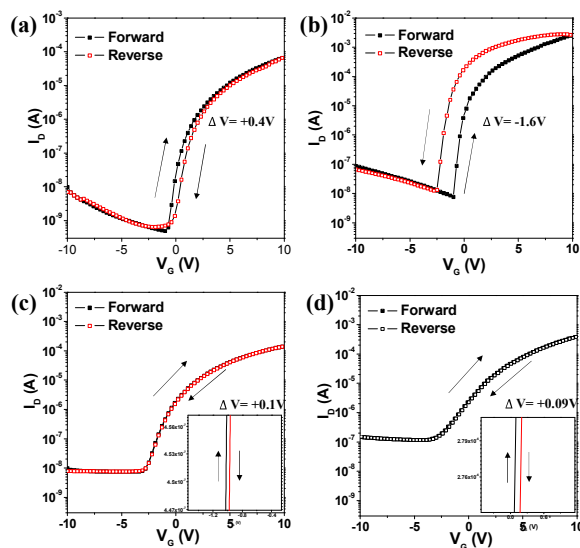


Fig. 4 Hysteresis behaviors of the In_2O_3 TFTs measured under the forward and reverse sweeping with (a) AO 250°C, (b) EG-AO 250°C, (c) EG-AO 350°C, and (d) EG-AO 500°C gate dielectric. Insets of (c) and (d) are enlarged pictures of each transfer curve.

almost identical, indicating that EG-related undecomposed residuals are decomposed with sufficient annealing time.

The chemical species of the residuals in the films were investigated by FT-IR (Fig. 3e and f). The vibration peaks related to NO_3 are assigned to $1200\text{--}1700\text{ cm}^{-1}$, and they originate from aluminium nitrate in both the AO and EG-AO precursor solutions.^{21,22} Nitrate groups are observed in films annealed at below 250°C and removed after 350°C due to thermal decomposition. A broad peak in the range of $3000\text{--}3500\text{ cm}^{-1}$ indicates hydroxyl groups ($-\text{OH}$) derived from hydrolysis of the precursor solutions. As the annealing temperature increases, condensation and dihydroxylation reactions become more active leading to a decrease in intensities of the hydroxyl-related peaks from the AO and EG-AO films.²³ A distinction between the AO and EG-AO films appears in the carbon-related peaks. The peaks at $2800\text{--}2900\text{ cm}^{-1}$ and $1000\text{--}1100\text{ cm}^{-1}$ correspond to the C-H and C-O vibration peaks, respectively.²³ The peak at $900\text{--}1000\text{ cm}^{-1}$ is attributed to the C-C stretching vibration.²⁴ Sharp and strong C-H, C-O, and C-C peaks are observed only in the EG-AO films prepared at 200°C and 250°C, and disappeared after 350°C. In contrast, none of the AO films showed carbon-related peaks. When the precursor solution containing EG is annealed under 250°C, EG is not fully decomposed and leaves carbon-related species, such as C-O, C-H, and C-C, in the films. Combining the results of the TGA and FT-IR analyses, it is concluded that the EG-AO film annealed at 250°C contains abundant EG-related carbon species.

Even though several literatures reported that hydroxyl and nitrate group induce the frequency-dependent capacitance, AO 250°C containing those shows constant capacitance over the entire range of frequency.^{17,19} Thus, EG residuals in EG-AO 250°C are the main reason for increase of capacitance at low

frequency. Under external applied bias, EG residuals are polarized and polar groups located at the end of EG residuals easily capture charge carriers, producing space charges inside AO film.^{14, 25} At a low frequency, the increase in capacitance due to space charge polarization results in a high current level of In_2O_3 TFT. As the frequency increases, the rotation of EG residual is interrupted due to friction against the AO matrix and charge carriers constructing space charges undergo macroscopic migration to change the orientation of polarization. Eventually, they cannot follow the field and, as a consequence, remain randomly oriented, resulting in a decrease in capacitance.

Observation of the hysteresis of the transfer curves further clarifies the EG residual in the AO layer acting as the source of the space charge polarization. Fig. 4 displays the hysteresis of the transfer curves of the samples under forward and reverse gate bias sweeps. The EG-free AO based In_2O_3 TFTs (see Fig. 4a, c and d) show clockwise hysteresis during the forward-reverse sweep; this is related to charge trapping at the channel/dielectric interface because the trapped electrons screen the applied gate field.²⁶⁻²⁷ In contrast, counter-clockwise hysteresis is observed in the EG-AO based In_2O_3 TFTs. During the forward gate bias sweep, the EG residuals are polarized according to the gate bias. As the reverse bias sweep begins, the change of the polarization lags behind the decreasing gate bias due to its restricted responding speed, *i.e.* slow polarization, retaining higher capacitance formed at high gate bias.²⁸ The higher capacitance generates higher current (Eq. 1) during reverse sweep than in the case of forward bias, which leads to counter-clockwise hysteresis.

Conclusions

In summary, we have investigated unusual high mobility of metal oxide TFT with solution-processed aluminum oxide gate dielectric. According to TGA and FT-IR analyses, EG in precursor solution is not fully decomposed and incorporated in the aluminum oxide layer at a low annealing temperature. EG residuals act as space charges, inducing frequency-dependent capacitance and leading to high capacitance at a low frequency. In this case, if the channel mobility is calculated with the conventional capacitance value at 1 MHz, it represents the severely overestimated value. Since TFTs operates in static condition, it is plausible to adopt the capacitance at 1Hz for the calculation of the channel mobility. Our conclusions may not apply to all studies on TFTs in which solution-processed Al_2O_3 gate dielectric with EG solvent. The mobility determined by frequency-dependent capacitance also depends on the maximum annealing temperature used during TFT processing, especially below 250°C.

Acknowledgements

This work was supported by the Materials Original Technology Program (10041222) funded by the Ministry of

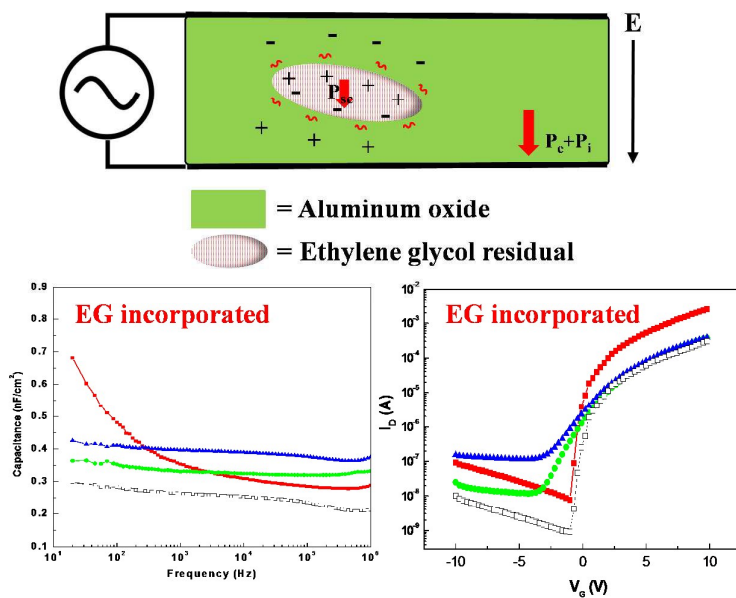
Trade, Industry and Energy of Korea and the National Research Foundation of Korea (NRF) grant funded by the Korea government (MSIP) (CAFDC 5-3, NRF-2007-0056090).

28 N. B. Ukah, J. Granstrom, R. R. Sanganna Gari, G. M. King, S. Guha, *Applied Physics Letters*, 2011, **99**, 243302

References

- 1 Y. Sun, J. A. Rogers, *Advanced materials* 2007, **19**, 1897
- 2 Y. H. Hwang, J. -S. Seo, J. M. Yun, H. Park, S. Yang, S. -H. Ko Park, B. -S. Bae, *NPG Asia Materials* 2013, **5**, e45
- 3 J. -S. Park, J. K. Jeong, M. Yeon-Gon, H. -D. Kim, S. -I., Kim, *Applied Physics Letters* 2007, **90**, 262106
- 4 P. Barquinha, A. M. Vila, G. Goncalves, L. Pereira, R. Martins, J. R. Morante, E. Fortunato, *IEEE Transactions on Electron Devices* 2008, **55**, 954
- 5 H. Q. Chiang, J. F. Wager, R. L. Hoffman, J. Jeong, D. A. Keszler, *Applied Physics Letters* 2005, **86**, 013503.
- 6 E. Fortunato, P. Barquinha, G. Goncalves, L. Pereira, R. Martins, *Solid-State Electronics* 2008, **52**, 443
- 7 Y. -L. Wang, F. Ren, W. Lim, D. P. Norton, S. J. Pearton, I. I. Kravchenko, J. M. Zavada, *Applied Physics Letters* 2007, **90**, 159
- 8 J.-S. Park, H. Kim, I.-D. Kim, *Journal of Electroceramics* 2013, **32**, 117
- 9 S. H. Kim, S. Nam, J. Jang, K. Hong, C. Yang, D. S. Chung, C. E. Park, W.-S. Choi, *Journal of Applied Physics* 2009, **105**, 104509
- 10 E. Lee, J. Ko, K.-H. Lim, K. Kim, S. Y. Park, J. M. Myoung, Y. S. Kim, *Advanced Functional Materials* 2014, **24**, 4689
- 11 L.; Zhang, J.; Li, X. W. Zhang, X. Y. Jiang, Z. L. Zhang, *Applied Physics Letters* 2009, **95**, 072112
- 12 J. H. Park, Y. B. Yoo, K. H. Lee, W. S. Jang, J. Y. Oh, S. S. Chae, H. W. Lee, S. W. Han, H. K. Baik, *ACS applied materials & interfaces* 2013, **5**, 8067
- 13 P. K. Nayak, M. N. Hedhili, D. Cha, H. N. Alshareef, *Applied Physics Letters* 2013, **103**, 033518
- 14 K. Song, W. Yang, Y. Jung, S. Jeong, J. Moon, *Journal of Materials Chemistry* 2012, **22**, 21265
- 15 C. Avis, J. Jang, *Journal of Materials Chemistry*, 2011, **21**, 10649
- 16 W. Yang, K. Song, Y. Jung, S. Jeong, J. Moon, *Journal of Materials Chemistry C*, 2013, **1**, 27
- 17 S. Jeong, J. Lee, S. Lee, Y. Seo, S.-Y. Kim, J. Park, B.-H. Ryu, W. Yang, J. Moon, Y. Choi, *Journal of Materials Chemistry C*, 2013, **1**, 4236
- 18 H.; Yue, Y.; Zhao, X.; Ma, J. Gong, *Chemical Society reviews*, 2012, **41**, 4218
- 19 J. H. Park, K. Kim, Y. B. Yoo, S. Y. Park, K.-H. Lim, K. H. Lee, H. K.; Baik, Y. S. Kim, *Journal of Materials Chemistry C*, 2013, **1**, 7166
- 20 B. N. Pal, B. M. Dhar, K. C. See, H. E. Katz, *Nature materials*, 2009, **8**, 898
- 21 J. Jose, M. J. Bushiri, K. Jayakumar, V. K. Vaidyan, V. S. Jayakumar, *AIP Conf. Proc.*, 2008, **1075**, 125
- 22 L. Djoudi, M. Omari, N. Madoui, *EPJ Web of Conferences*, 2012, **29**, 00016
- 23 B. Chieng, N. Ibrahim, W. Yunus, M. Hussein, *Polymers*, 2013, **6**, 93
- 24 B. Helina, P. Selvarajan, A. S. J. Lucia Rose, *Physica Scripta*, 2012, **85**, 055803
- 25 S. C. Lim, S. H. Kim, J. B. Koo, J. H. Lee, C. H. Ku, Y. S.; Yang, T. Zyung, *Applied Physics Letters*, 2007, **90**, 173512
- 26 C. S. Kim, S. J. Jo, S. W. Lee, W. J. Kim, H. K. Baik, S. J. Lee, *Advanced Functional Materials*, 2007, **17**, 958
- 27 J. Liu, D. B. Buchholz, J. W. Hennek, R. P. H. Chang, A. Facchetti, T. J. Marks, *Journal of the American Chemical Society*, 2010, **132**, 11934

TOC GRAPHICS



Undecomposed ethylene glycol residuals in solution processed aluminum oxide gate dielectric results in the frequency-dependent capacitance.